frontiers | Frontiers in Environmental Science

TYPE Original Research
PUBLISHED 01 September 2022
DOI 10.3389/fenvs.2022.971786

OPEN ACCESS

EDITED BY
Snehasis Kundu,
National Institute of Technology, Jamshedpur, India

REVIEWED BY
Weilin Chen,
National University of Singapore, Singapore
Xuanlie Zhao,
Harbin Engineering University, China

*CORRESPONDENCE
Liqin Zeng,
zlq_pbl@126.com

SPECIALTY SECTION
This article was submitted to Freshwater Science, a section of the journal Frontiers in Environmental Science

RECEIVED 17 June 2022
ACCEPTED 03 August 2022
PUBLISHED 01 September 2022

CITATION
Liu M, Zeng L, Wu L, Zhu C and Abi E (2022), Effect of periodic water-sediment laden flow on damage for steel piles.
Front. Environ. Sci. 10:971786.
doi: 10.3389/fenvs.2022.971786

Effect of periodic water-sediment laden flow on damage for steel piles

Mingwei Liu, Liqin Zeng*, Linjian Wu, Chenhao Zhu and Erdi Abi

National Engineering Research Center for Inland Waterway Regulation, School of River and Ocean Engineering, Chongqing Jiaotong University, Chongqing, China

Due to the problems of shallow overburden and deep water construction, etc., steel tube piles are mostly used in the substructures of frame-wharves in inland rivers of China, especially in the upper stream of Yangtze River. Affected by the fluctuating backwater area of the Three Gorges, anticorrosion coatings of steel structures generally fell off. The steel piles exposed to the water level fluctuation area are subjected to periodic erosion damage process of water-sediment laden flow, which accelerate the corrosions of the steel pile and greatly affect the durability of the wharf structures. In order to explore the effect of periodic water-sediment laden flow on the damage for steel piles in water level fluctuation area of inland rivers, a series of accelerated periodic erosion tests were carried out in laboratory to acquire the damage laws of steel samples under different working conditions. Results showed that the residual masses of steel samples fluctuated with the increasing number of cycles and that the corrosion depths of steel samples were logarithmically correlated with the experimental time. According to the results of periodic accelerated erosion test based on the water-sediment laden flow and existing corrosion theory, a time-dependent model for the corrosion of steel components under water-sediment laden flow was established, as well as a evaluated method for the resistance degradation of steel pile was proposed. Finally, after 20 years, the actual resistance of the steel structure exposed to the water level fluctuation area was less than 60% compared by the initial structural resistance. The research results can provide important guiding significance for reasonably predicting the durability of hydraulic steel structures.

KEYWORDS

water-sediment laden flow, periodic erosion, steel piles, damage, resistance deterioration

Introduction

Affected by the fluctuating backwater area of the Three Gorges, the multi-layers frame-type wharf structures are mostly used in the upper stream of the Yangtze River. The substructures of these structural types usually adopt the steel structures with high strength, light weight and convenient construction. As the steel structure (Including longitudinal and transverse steel braces, steel berthing component, steel tube) under the wharf is eroded by water-sediment laden flow year round, the anticorrosion coating of the

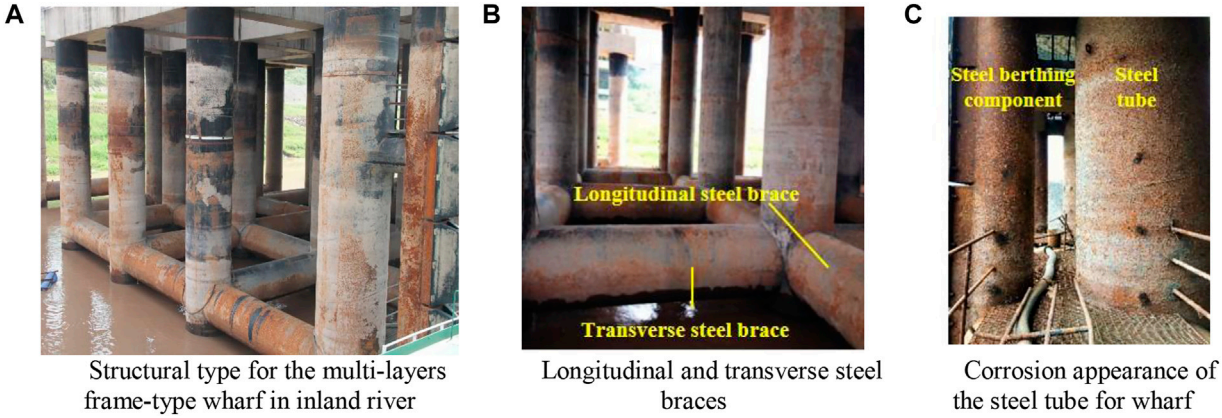

FIGURE 1
Damage morphology of the steel components for the multi-layers frame-type wharf in inland river (Steel component include longitudinal and transverse steel braces, steel berthing component, steel tube).

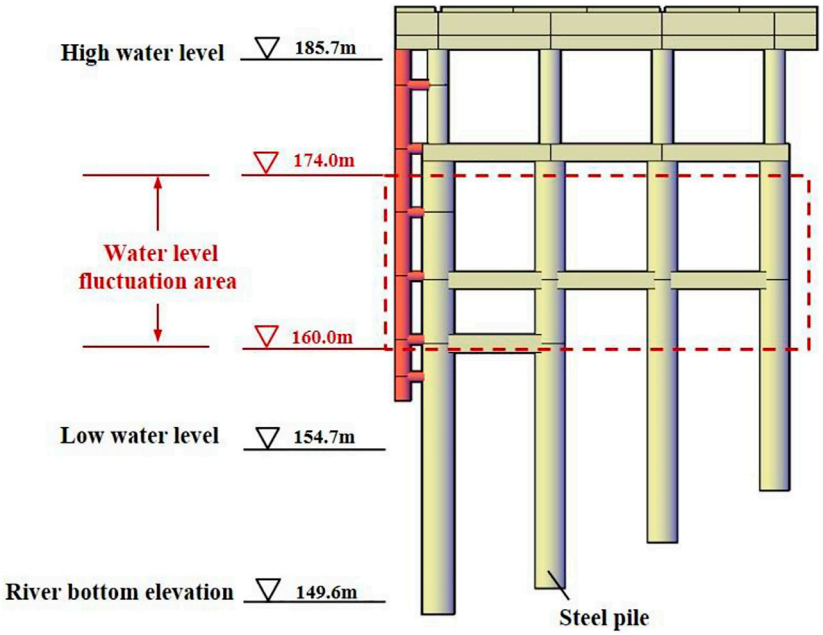

FIGURE 2
The elevation of water level fluctuation area for the multi-layers frame-type wharf in inland river.

steel components have been generally fallen off, as shown in Figure 1. Exposed steel substrates are prone to periodic erosion, which located in the water level fluctuation area (Figure 2).

In the drying stage, the oxygen supply is sufficient under the action of a liquid membrane, and the accumulation of erosive ions is enriched (Thee et al., 2014); under an immersed condition, the corrosion products of steel components dropped off due to the erosion by water-sediment laden flow, and the steel substrate is exposed again. The alternating process of drying and wetting accelerates the corrosion rate of steel components. According to statistic data, the annual total loss of metal due to corrosion processes in the world exceeds 10% account for its annual production (Panteleeva, 2017). The major consulting project of "Research on Chinese corrosion status and control strategy" showed that Chinese annual corrosion cost accounted for about 3.34% of the gross domestic product (GDP) in 2014 (Zhang et al., 2022). The corrosions of steel components have attracted increasing attention.

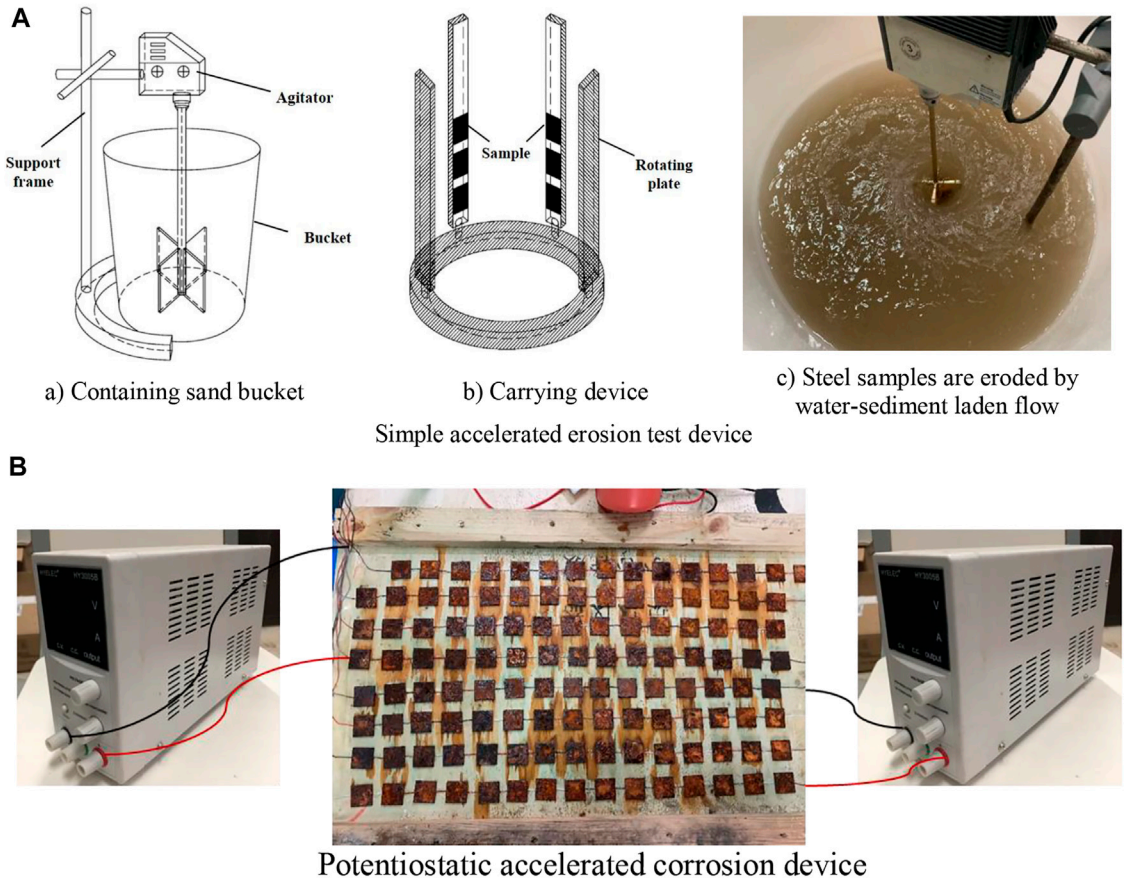

FIGURE 3
Accelerated test devices. Simple accelerated erosion test device include containing sand bucket and carrying device. The sand bucket consists of agitator, support frame, and bucket.

On the basis of field investigations, it was found that the average corrosion rate of steel components of a large wharf exposed to the water level fluctuation area in the upper reaches of the Yangtze River is approximately 0.27 mm/a, the average corrosion rate of steel ones exposed to the atmospheric area is approximately 0.025 mm/a (Wang et al., 2021), and the average corrosion rate of steel structures exposed to the spray/splash area in marine environment is approximately 0.3 mm/a (Jiang et al., 2021). The corrosions of steel structures are very serious in the drying-wetting environment in inland rivers, which can directly affect the durability and safety of steel structures.

The corrosion behaviours of steel structures in marine environments and atmospheric environments have attracted much attention. The splash zone in marine environments has its impact characteristics of high humidity, high salt spray, and frequent wave (Gabreil et al., 2022). Compared with other exposure environments, the corrosion degree of steel components in the splash zone is more serious (Xu et al., 2021). The metal surface is subjected to drying-wetting cycle for a long time under marine environmental conditions, and the chloride ions will accelerate the corrosion rate of the metal (Melchers, 2020). For the atmospheric corrosion of steel, a layer of water film is first adsorbed on the surface of steel (the relative humidity of air is less than 100%); When the thickness of the water film reaches 20–30 molecular layers, electrochemical corrosion under the electrolyte film will occur, subsequently, further form a dense protective rust layer (Zhang, 2019). Many scholars have conducted in-depth explorations on the corrosion behaviours of steel structures under the alternate drying and wetting conditions. Gong et al. (2020a), Gong et al. (2020b) found that the thickness of the rust layer formed in a drying-wetting cycle was larger than that in a soaked environment during the same corrosion time. Results indicated that the drying-wetting cycle was conducive to the rapid formation of the rust layer, and a larger drying-wetting ratio was more likely to result in corrosion and cracking for steel. Hao et al. (2018) studied the electrochemical characterization and stress corrosion cracking (SCC) behaviour for high strength steel in marine environment under drying-wetting cycles and found that the corrosion layer has an impact on the electrochemical and

SCC behaviours. Wang et al. (2021) simulated the atmospheric corrosion evolution process for the low-carbon steel in coastal atmosphere, and the results showed that with the increasing dry-wet cycles, the corrosion rate increased rapidly at first and then slowly until it reached a plateau. However, for the exposure environment in inland rivers, it has strongly differences than those of the aforementioned corrosion environments. According to the water quality analysis for the inland river environment, the chloride content is only 14.5 mg/L, hence, the influence of chloride ions on the corrosion of steel structures can be reasonably ignored. Moreover, the service environment of inland river has its characteristics of a high flow rate and high sediment content during the flood season. After the anticorrosion coating on the surface of steel components fallen off, the corrosion products produced by the steel base material will be continuously eroded by the water-sediment laden flow. The water level of the steel components in wharf rises and falls periodically with the variation of seasons, and the corrosions for steel structures will be accelerated by the alternate drying-wetting conditions.

Periodic erosion on steel structures by water-sediment laden flow will not only weaken the effective bearing area for steel components, but also reduce the strength, plasticity and other major mechanical properties of steel structures, resulting in a decline for the bearing capacity of steel structures (Luo L et al., 2019; Goran et al., 2021). Luo X et al. (2019) showed that the average corrosion rate can effectively reflect the degradation of the bearing capacity for corroded steel bars but do not accurately reflect the degradation of their deformation and capacity. Zhan et al. (2018) used the model of random process to characterize the initial bearing capacity, degradation of geometric parameters and mechanical properties for the corroded steel components and established a degradation model for corroded ones based on the mathematical statistics theory. Zou et al. (2019) established a prediction probability model for the resistance degradation of corroded steel structures exposed to a chlorine-salt environment by using the Monte-Carlo simulation method and found that the initial corrosion time for steel follows a lognormal distribution, and the structural resistance at the same time can be represented by a normal distribution. Sultana et al. (2015) used the finite element method to analysis the influence of random corrosion on the compressive strength of steel structures, and reported that a volume loss of approximately 18% would lead to 45% reduction in the ultimate strength of steel. Zhao et al. (2021) studied the influence of random pitting on the bending capacity of H-shaped steel beams and found that the mass loss and corrosion depth would both affect the bearing capacity of steel components. At present, the resistance degradation model mainly focuses on concrete/reinforced concrete structures, while researches on the resistance degradation model for steel ones under drying-wetting cycles are very limitation and are worthy of further researches and explorations.

TABLE 1 Accelerated corrosion test conditions for steel samples.

Condition name	1	2	3	4	5
Erosion speed (m/s)	1.29	1.71	2.18	2.18	2.18
Sediment concentration (kg/m^3)	4.5	4.5	4.5	20	0.0

In summary, researches regarding the corrosion laws for steel structures mostly resided in the marine and atmospheric environments. To date, there are few reports on the effect of periodic water-sediment laden flow on damage of steel structures under the water level fluctuation area in inland river. Therefore, it is still necessary to carry out relevant researches aimed to the aforementioned problems. According to the characteristics of large flow velocity and high sediment concentration in inland rivers, the indoor accelerated test method was carried out to simulate the periodic erosion water-sediment laden flow acted on steel samples, and the corrosion evolution laws for the steel structures under the water level fluctuation area were revealed, as well as the resistance degradation model for the steel was established to provide a theoretical basis for the anticorrosion design of steel structures.

Cyclic accelerated erosion test under water-sediment laden flow

Experimental devices

Samples preparation

In this test, the Q235 steel block with a size of 3 cm × 3 cm × 0.2 cm (length × width × height) was used to polish the steel surface to class St3 in accordance with "Corrosion Grade and Rust Removal Grade of Steel Surface Before Painting" (State Bureau of Technical Supervision GB8923-88, 2011), and then the steel surface should be wiped clean with alcohol and dried for later use. A total of 150 specimens were prepared for this paper's experiment.

Accelerated test device

Han et al. (2014) studied the initial corrosion behaviors of carbon steel under the field and indoor drying-wetting cycles and found that the corrosion behaviors under both the conditions follow the mathematic equation of $D = At^n$. The indoor corrosion rate by drying-wetting cycles was three times than that of the field test, and these two kinds of conditions had a good correlation. Therefore, we can obtain the corrosion law of steel samples in inland river environments during a short time by the accelerated test. The experimental devices developed by our research group were used during the accelerated test for steel samples, as shown in Figure 3.

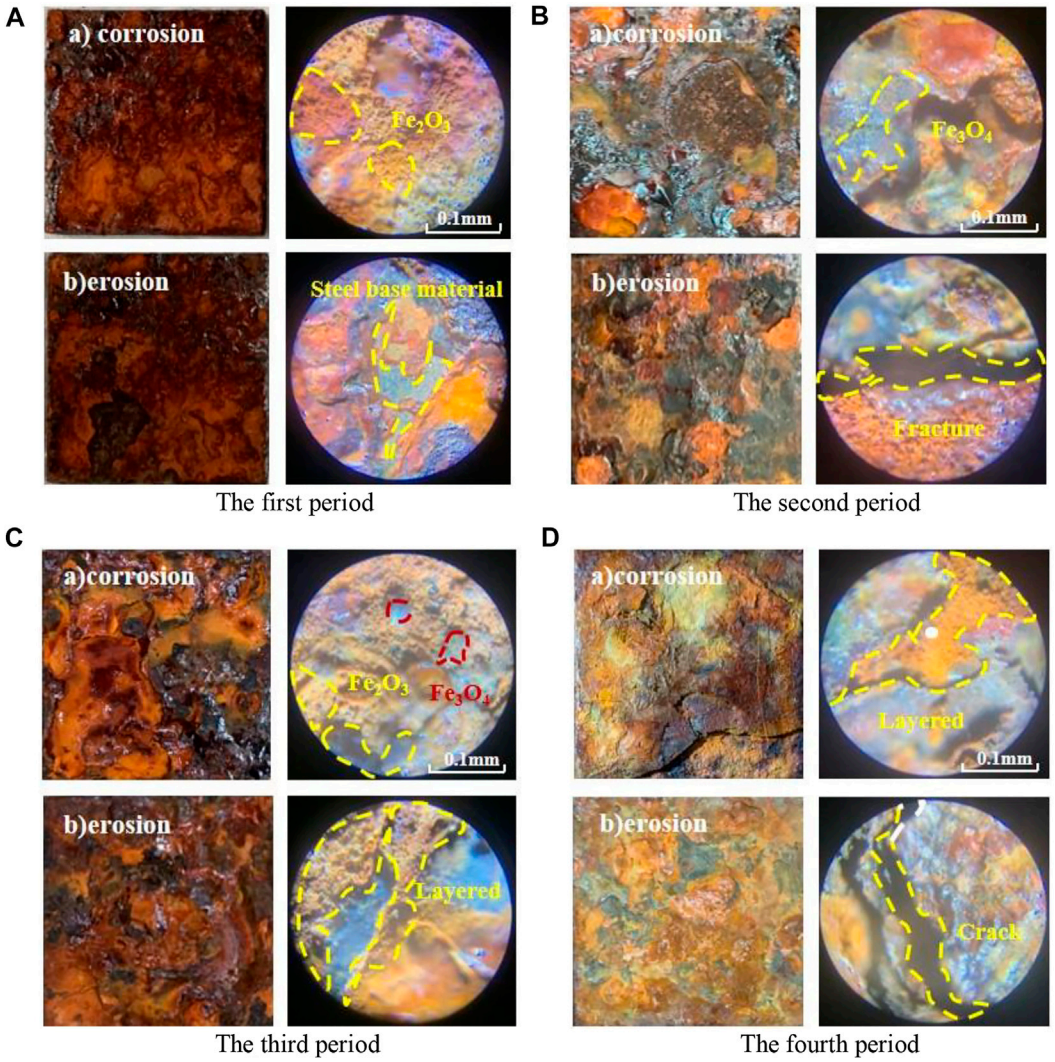

FIGURE 4
Damage morphology of steel samples under periodic water-sediment laden flow. **(A)** The first period. **(B)** The second period. **(C)** The third period. **(D)** The fourth period.

(1) Simple accelerated erosion test device: this device comprises a sand bucket (Including agitator, support frame, bucket) and a carrier, and the carrier is put into the sand bucket to form a complete set of instrument. The device obtains muddy water with different sediment concentrations by manual operation, adjusts the rotating speed of the test machine, simulates different erosion speeds, and obtains sand water flow under different flow velocity conditions. This instrument can be used to explore the erosion change law of steel samples under different erosion conditions, including erosion time, erosion speed, sediment concentration, etc. Moreover, the stirring rods for the experimental device have been improved that the experimental steel samples are placed/installed in the stirring rods, as shown in Figure 3A.

(2) Potentiostatic accelerated corrosion device: the HY3005B direct current (DC) power supply provides an external current for the whole system. The humidifier continuously sprays water mist to create a high humidity environment and form a water film on the steel surface. The steel samples are connected with the DC power supply by wires to form a closed loop, as shown in Figure 3B. At the same time, double-sided adhesive, wood and foam materials are used to fix the position of the steel samples. The corrosion rates of the steel samples are changed by setting the current value, recording the corrosion time, and then weighing and measuring the thickness of the steel samples every 30 h. The current value of this test is set as 25 mA. According to the current distribution law of series and parallel circuits (see in Figure 3B), if we

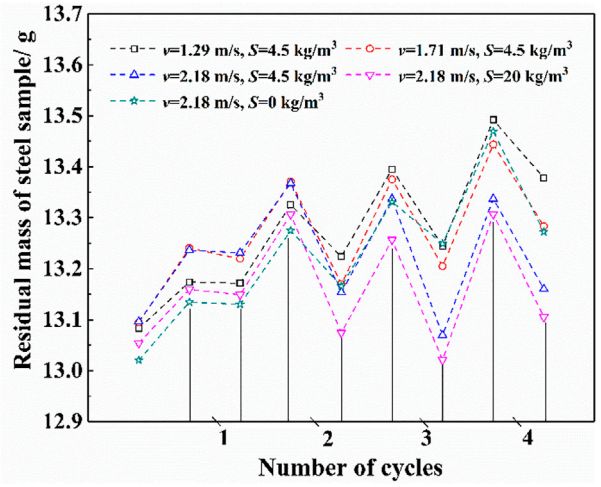

FIGURE 5
Variation of steel sample residual mass with cycle number (each cycle contains corrosion and erosion process).

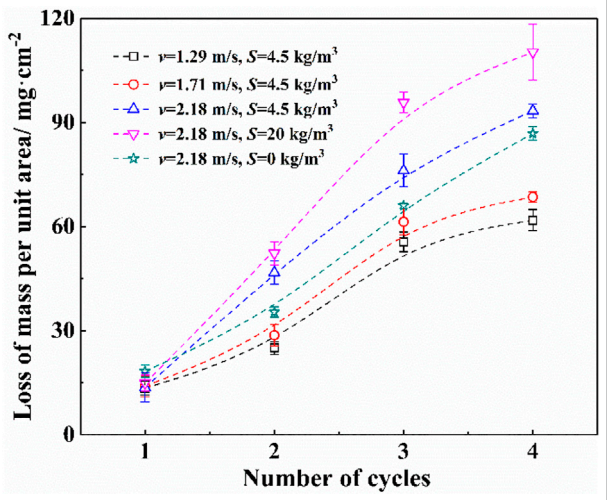

FIGURE 6
Loss of mass per unit area for the steel samples versus the number of cycles.

ignore the heterogeneity between test pieces, the current flowing through each steel sample is consider as 5 mA.

Test plan

Corrosion characteristics of steel structures are mainly related to environmental conditions, dry/wet ratio and exposure time, as well as the flow velocity and sediment concentration of water-sediment laden flow. According to the tested flow velocity of 0.6–3.0 m/s in the middle and upper reaches of the Yangtze River (Shen, 2015), hence, the flow velocities for this paper's experiment are determined from 1 to 2 m/s, as 1.29 m/s, 1.71 m/s and 2.18 m/s, respectively, which represent the minimum, the average, and the maximum flow velocity during the flood season. The erosion velocities by water-sediment laden flow can be adjusted by changing the rotational speed of the rotary head of the simple accelerated erosion test device.

For this paper's experimental investigations, the sediment concentrations are considered as 4.5 kg/m^3 and 20 kg/m^3 on the basis of the tested sediment concentration in the middle and upper reaches of the Yangtze River. According to the pre-test results, the corrosion quality for steel samples hardly increase after the accelerated corrosion time reaches to 150 h, and the loose rust layer on the steel surfaces is almost washed away after erosion for 2 h. Therefore, each accelerated corrosion time and each accelerated erosion time are determined as 150 and 2 h, respectively, with a total of 4 cycles. A total of 6 parallel samples are set for each cycle test, and a total of 150 parallel samples are prepared in this paper's experiment.

Five working conditions are designed according to the field design conditions, as shown in Table 1.

Test results

The corrosion indices for steel samples mainly include mass loss (Zheng et al., 2018), corrosion rate (Song et al., 2021; Wang and Liu, 2021), corrosion depth (Wang and Cheng, 2016), corrosion products (Chen et al., 2021), corrosion morphology (Ming et al., 2022), fractal characteristics (Ren et al., 2022a), roughness (Xu and Wang, 2015), time-dependent model for the rust pit depth to diameter depth ratio (Ren et al., 2022b), etc. This paper focuses on an analysis of corrosion morphology, mass loss, corrosion depth, and other indices. The surface morphology of steel samples is photographed and recorded by a high definition camera (HDV). The masses of steel samples after the process of corrosion and erosion are measured by using a BSM120.4 electronic analytical balance (accurate to 0.1 mg). The masses are weighed as least five times, and the average values are taken as the final mass values. A T112 ultrasonic thickness gauge is used to measure the thickness of steel samples after corrosion and erosion test. The thicknesses are measured at least five times for each sample, and the average values are considered as the final results.

Results

Effect of periodic water-sediment laden flow on damage morphology of steel samples

During the process of periodic water-sediment laden flow, a dense layer of corrosion products is formed on the steel

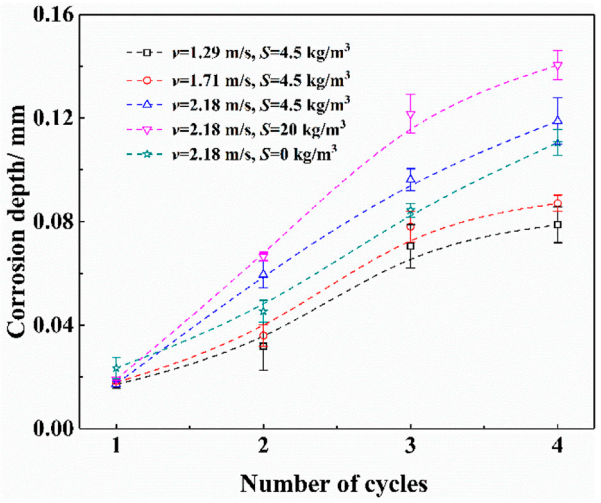

FIGURE 7
Steel corrosion depth versus the number of cycles.

surface by accelerating the current under a high humidity environment, and some of the corrosion products drop off due to the impact and abrasion caused by water-sediment laden flow. After four cycles, a rust layer with a certain apparent strength is generally formed on the steel surface, and the quality of rust product hardly increases. Therefore, four cycles of the alternant washout-corrosion tests are determined.

(1) The first period. The early and unstable rust layer formed on the steel surface is a mixture of ferric oxide (Fe_2O_3; containing crystal water is yellow, losing crystal water is red brown), especially, the rust layer structure and the rust product are loose, and the adhesion strength of corrosion products is low. Early rust products are loose and porous, which demonstrate strong water absorption, low strength, brittleness, easily erosion by water-sediment laden flow and flake off. After the rust layer flakes off, the original steel matrix can expose to a corrosive atmosphere again, as shown in Figure 4A.

(2) The second period. After exposure to the first cycle test, a relatively dense oxide layer is formed on the steel surface, which isolates the rust causing conditions to a certain extent and protects the steel surface. At this stage, the rust products gradually change from the initial iron oxide to ferroferric oxide (Fe_3O_4; black color), and the surface volume expansion of the rust layer is particularly obvious. After the impact of water-sediment laden flow, the damage and shedding of the rust layer mostly occur at the volume expansion, and there are obvious cracks at the falling place. There is a large gap between the cracks, which provides a channel for water and air to enter the steel base material, so that the corrosion reaction on the inner surface of steel can be still occurred slowly, as shown in Figure 4B.

(3) The third period. The surface of the rust layer which almost not fell off is dark black from the macroscopic morphology of the rust layer, which has high strength, good compactness and a certain protective effect on steel corrosion. The surface after the rust layer falling off shows yellow and reddish brown, which is relatively loose and porous. The erosion damage of the samples mainly occurs in this area, and the rust products have obvious stratification after several "drying-wetting cycles", as shown in Figure 4C.

(4) The fourth period. The residual rust layer on the inner surface overlapped with the newly formed rust products on the outer surface, and the rust layer surface showed obvious stratification and brittle fracture characteristics. From the macroscopic morphology, the rust layer on the steel surface has begun to denude the whole block. From the microscopic morphology of steel samples, the surface rust layer has obvious cracks after repeated wetting and drying cycles. Most of the cracks are caused by the composition, and the growth degree and integrity of the inner and outer rust layers are not consistent. Due to multiple cycles, the rust layer is divided into multiple layers from inside to outside, which has poor cementation ability and prone to relative sliding. The strength of the surface rust layer is weaker than that in early stage, and it is more likely to be damaged and fall off in a large area under a high flow velocity, as shown in Figure 4D.

In summary, a large number of loose corrosion products appear on the steel surface in the early stage of the periodic erosion process under water-sediment laden flow. In the middle stage, loose rust products will fall off and gradually stratify into rust layer. Subsequently, the rust layer on the steel surface will fall off, and a dense rust layer will form inside, which will inhibit the entry of external media. Therefore, the periodic erosion process of water-sediment laden flow can promote the formation and stabilization of a compact and thick inner rust layer of steel samples, thus slowing down the corrosion rate.

Effect of periodic water-sediment laden flow on mass loss of steel samples

The cyclic damage process of steel samples is mainly affected by the damages of atmospheric corrosion and water-sediment laden flow erosion. Under five different working conditions, the variation curve of the residual masses of the steel samples with the number of cycles are exhibited in Figure 5.

Figure 5 shows that the residual masses of the steel sample fluctuate with an increased cycles. In atmospheric environment, steel combined with atmospheric water vapor and oxygen forms hydration oxidation products, so that the quality of steel samples

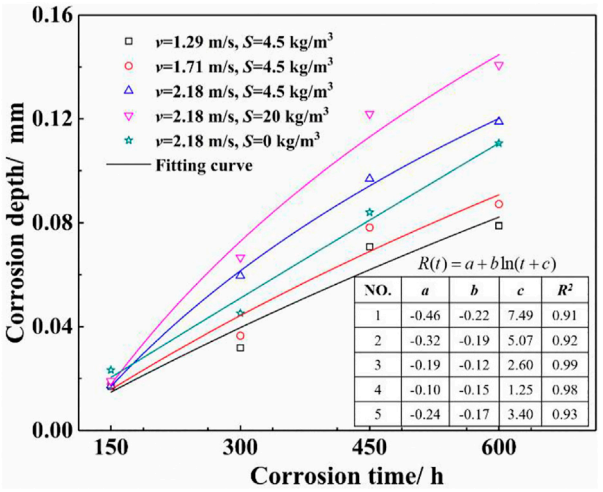

FIGURE 8
Fitted curves of steel corrosion depth with corrosion time.

increases. The quality decline of steel samples is caused by the erosion of corrosion products on the steel surface under the condition of water-sediment laden flow. Therefore, the qualities of the steel samples fluctuate up and down with the experimental cycles.

When the flow velocity is relatively low (1.29 m/s and 1.71 m/s), the residual masses of the steel samples show a slow rising trend with the cycles. This is because that the loose corrosion products on the steel surface are easily washed by the slow flow, while the relatively dense oxidation products are difficult to damage and cannot easily fall off. Therefore, the residual masses of the steel samples show a slow rising trend. At a relatively large flow velocity (2.18 m/s), the rust layer on the steel surface has difficulty remaining intact under the erosion of water-sediment laden flow. The damaged surface and cracks of the rust layer easily provide channels for water vapor to penetrate, and further rust occurred. The rust layer is loose and porous, and the corrosion products interact with each other, which can easily cause damage and spalling in the next erosion. Therefore, the quality of steel components is always dynamically stable with a certain downward trend.

In summary, the residual masses of the steel samples are relatively stable even though they fluctuate exposed to the water level fluctuation zone. On the condition of low sand content or low flow rate, the internal rust layer is not easily washed away, and the exposed steel matrix and interfacial void on the steel surface easily grow the rust layer again. Therefore, the rust layer accumulates slowly, so the residual masses of steel samples rise slowly. On the condition of medium and high sand content or high flow rate, the rust layer of steel members can be easily eroded and damaged, and the corrosion products have difficulty accumulating. Therefore, the quality of steel samples remains dynamic and stable and tends to decrease with the increasing cycle times.

At the end of each cycle, the rusts on the surface of the sample are polished to remove; subsequently, the remaining masses for steel samples are weighed, and the unit weight losses of the samples are recorded. The damage rule of steel samples under different working conditions and the variation process of unit weight loss for samples with the cycles are confirmed, as shown in Figure 6.

Figure 6 exhibits that the unit mass loss of the steel sample with the number of cycles verifies as an initial rapid increase and then slow increase, which is consistent with a logarithmic growth law. Moreover, we can observe that:

(1) On the condition of the same sediment concentration, the unit mass loss of the rust layer increases with the increasing flow velocity.
(2) On the condition of the same flow velocity, the unit mass loss of the rust layer increases with the increasing sand concentration.
(3) As the cycling times increase, the unit mass loss of steel samples gradually slows because that the first three loop component surfaces are mainly composed of a loose rust layer of steel, which is vulnerable to erosion from falling out.
(4) After several cycles, a rust layer with certain apparent strength gradually formed on the steel surface, and the loss of unit mass for steel samples under the fourth cycle is smaller than that of the first three cycles, which is consistent with the steel surface morphology damages.

Effect of periodic water-sediment laden flow on thickness loss of steel samples

The variation of steel corrosion depths with the number of cycles on the conditions of five water flows are elaborated in Figure 7.

Figure 7 states that the corrosion depths of the rust layer on the steel surface with the number of cycles generally change as an initial rapid increase and then a slow increase, which is consistent with the trend of steel loss mass. On the basis of the change law for steel corrosion depths combined with the apparent morphology analysis of steel samples, it can be concluded that:

(1) In the early stage of erosion, the rust layer newly formed on the steel surface is closely attached to the surface of the base-material and it is relatively dense and difficult to wash out. However, the rust layer surface has not formed certain strength, and the loose rust products can be easily washed off, so the steel damage during the early stage of the cycle is less, and the erosion depth is small.

FIGURE 9
Corrosion results for steel components of a certain wharf tested in field.

TABLE 2 Steel corrosion results measured at a certain wharf in the upper reaches of Yangtze River units: mm.

Corrosion depth name of the structure	2013	2019		2021	
	Original thickness	Average remaining thickness	Average corrosion depth	Average remaining thickness	Average corrosion depth
Steel braces	20.00	19.21	0.79	18.92	1.08
Steel berthing components	16.00	15.32	0.68	14.94	1.06
Steel tubes	16.00	15.26	0.74	14.98	1.02
Average values	17.33	16.60	0.73	16.28	1.05

(2) After a certain period of drying and wetting circulation, the rust layer on the steel surface is scoured by water, and part of them would be fallen off. The rust layer has discontinuous growth, stratification, overlapping, gaps and other defects between the layers, as well as the layer is mixed with fine sediment particles. The rust layers would be easily fallen off from blocks under the current erosion. Therefore, in the middle of the cycle, the steel erosion damages are more serious than those of the early stage, and the erosion depths reach to peak values.

(3) At the later stage of the cycle, the rust layer acquired certain strength after repeated washout-corrosion cycles. It is difficult to cause large area damage and fall off for the rust products due to the water flow, but some corrosion products in steel surface can still fall off under the action of washout. Therefore, the increase in erosion thickness of steel samples tends to be slowed down at the late cycle.

Resistance degradation model of steel components

The corrosion damage of steel can not only weaken the effective bearing area of steel structures but also change the steel material properties. Moreover, the strength and safety for the steel components would be reduced, and the resistance degradation process of the steel structure can be accelerated. For this paper's study, a resistance degradation model for the steel components is established to describe the relationship between the steel strength weakening with the service time, which can strongly provide the theoretical supports for life prediction and safety evaluation of the wharf steel structures in inland river.

First, the time-dependent model for the steel corrosion depth is determined. The empirical formula for predicting the corrosion depth of steel components under different working

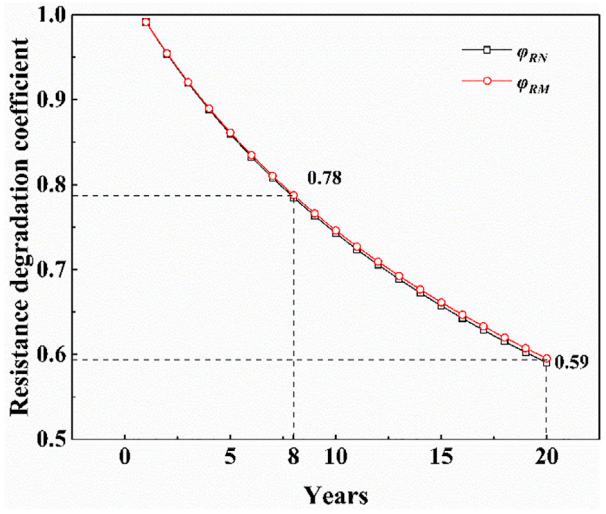

FIGURE 10
Resistance degradation coefficient of the steel components.

conditions is confirmed by fitting the variation trends of the average corrosion depth of steel samples with corrosion time, as shown in Figure 8.

As shown in Figure 8, a logarithmic function is used to fit the scatters, and the fitting correlation is relatively high. Therefore, the function relation of $R(t)$ is finally determined as follows:

$$R(t) = a + b\ln(t + c) \tag{1}$$

In Eq. 1, $R(t)$ is the corrosion depth of the steel component at t years, mm; t is the steel corrosion time, year; a , b and c are normalized parameters and can be determined according to the specific environmental conditions.

We obtain the dimensionless parameters in Eq. 1 according to engineering examples. At the end of 2013, a certain wharf in the upper reaches of the Yangtze River has been operated approximately 8 years. A large number of experimental data in line with the damage of steel components, such as piles, braces, beams, etc., caused by periodic water-sediment laden flow were collected in the field, as shown in Figure 9.

The average corrosion depths for wharf steel components were determined by combining relevant literatures and on-site actual detection measurements, as listed in Table 2.

Assuming that the effective protection life of the anticorrosion coating of steel components is 3 years, the corrosion time of steel components is 4 years. According to the average values for steel components determined in 2013, 2019, and 2021 as exhibited in Table 2, the parameters of a, b, and c are comfirmed by using the Eq. 1, and their calculated results are eqaul to 0.3092, 0.3433, 0.4063, respectively. The prediction model of steel corrosion depth can be obtained as follows:

$$R(t) = 0.3092 + 0.3433\ln(t + 0.4063) \tag{2}$$

In Eq. 2, $R(t)$ is the corrosion depth of the steel component at t years, mm; t is the steel corrosion time, year.

Shi et al. (2012) proposed the time-dependency of steel material strength weakening, and its expression is as follows:

$$f_t = [1 - 0.98w_s]f = \left[1 - 0.98\frac{A_0 - A_t}{A_0}\right]f \tag{3}$$

Where, f_t is steel material strength design value at the certain time t, N/m^2; w_s is the corrosion damage factor; f is the corroded steel strength design value (if the steel material for the significant components is Q235, the f= 235 N/m^2); A_0 is the initial section area of steel component, mm^2; and A_t is the actual section area of steel component corroded at time t, mm^2; $A_t = A_0 - \pi DR(t)$, D is outer diameter of steel components, m.

The degradation model for the design bearing capacity of steel components under the tension or compression is as follows (Fan et al., 2009):

$$N_R = A_t \cdot f_t = A_0 f \varphi_{RN} \tag{4}$$

Where, N_R is the axial bearing capacity, N; φ_{RN} is the design bearing capacity degradation coefficient of the steel ring section under the tension and pressure. Inserting the Eq. 3 into Eq. 4, the design bearing capacity degradation coefficient of the steel ring section under the tension and pressure is established.

$$\varphi_{RN} = k \cdot [R(t)]^2 - 0.1 \cdot R(t) + 1 \tag{5}$$

Where, $k = 2.52 \times 10^{-3}$, it can be determined according to the specific environmental conditions.

The flexural bearing capacity degradation model for the main plane of steel components is (Fan et al., 2009):

$$M_R = W_t \cdot f_t = W_0 f \varphi_{RM} \tag{6}$$

Where, M_R is flexural capacity, N·m; W_t is bending section coefficient at time t, m^3; φ_{RM} is the degradation coefficient for the main plane flexural bearing capacity of the ring section. Inserting the Eq. 3 into Eq. 6, the degradation coefficient for the main plane flexural bearing capacity of the ring section is confirmed.

$$\varphi_{RM} = \frac{1500 \cdot \varphi_{RN}}{1500 - 2 \cdot R(t)} \tag{7}$$

According to Eqs 5, 7, the time-dependent formulas for the degradation coefficient φ_{RN} and φ_{RM} are drawn, as shown in Figure 10.

From Figure 10, assuming that no anticorrosive measures are taken on the steel surface exposed to the water level fluctuation area, and the uniform corrosion process of steel components are considered, the bearing capacity of the ring steel components decays to 78% account for its initial resistance after 8 years. After the design corrosion life is reached, the bearing capacity degradation of the steel components is accelerated. After

20 years' service, the actual resistance of the steel structure is less than 60% compared by the initial value.

Conclusion

In this paper, the damage process of wharf steel components is simulated during the service environment of periodic erosion/corrosion by water-sediment laden flow in inland river, as well as the time-varying laws of morphology damage, mass loss and erosion depth of steel samples are obtained and analyzed. The prediction model of steel corrosion under periodic erosion/corrosion by water-sediment laden flow is finally established, and the evaluation method of resistance degradation of wharf steel components is proposed.

(1) At the initial stage of the steel damage test by periodic water-sediment laden flow, the steel surface is mainly composed of a loose rust layer, which can be easily eroded off. In the middle stage of the test, the rust products exhibit obvious stratification phenomena. At the later stage of the test, the rust layer on the steel surface begins to denude over the whole piece, and the steel surface forms a certain apparent strength, which can prevent rust and erosion for the steel structures.
(2)]At the water level fluctuation area, especially, in the upper reaches of the Yangtze River, the corrosion of steel components results in an increase in mass. The mass of the steel components decreases with the rust layer washing out by the water-sediment laden flow. Therefore, the residual mass of the steel components shows a continuous fluctuation, and the fluctuation trend slows down with the increasing flow velocity and sediment concentration. These findings are consistent with the steel surface morphology damage.
(3) On the basis of the research results by this paper, an evaluation method for resistance degradation of steel components under the periodic erosion/corrosion of water-sediment laden flow is proposed. The estimation results show that the actual resistance of the steel structure exposed to the water level fluctuation area in the upper reaches of the Yangtze River is less than 60% compared by the structural initial value after 20 years.

Data availability statement

The original contributions presented in the study are included in the article/supplementary material, further inquiries can be directed to the corresponding author.

Author contributions

Conceptualization, ML; methodology, ML and LZ; validation, LW; formal analysis, CZ and LW; investigation, EA; resources, ML; data curation, LZ and CZ; writing—original draft preparation, ML and LZ; supervision, LW All authors have read and agreed to the published version of the manuscript.

Funding

This research is funded by the National Natural Science Foundation of China, project number: 51479014, and the Talents Plan Project in Chongqing of China, project number: cstc2021ycjh-bgzxm0053.

Conflict of interest

The authors declare that the research was conducted in the absence of any commercial or financial relationships that could be construed as a potential conflict of interest.

Publisher's note

All claims expressed in this article are solely those of the authors and do not necessarily represent those of their affiliated organizations, or those of the publisher, the editors and the reviewers. Any product that may be evaluated in this article, or claim that may be made by its manufacturer, is not guaranteed or endorsed by the publisher.

References

Chen, W., Jiao, X., Zhao, Z., Li, H., Liu, R., and Che, Y. (2021). Study on salt spray corrosion behavior and mechanism of hot dip galvanized steel. *J. Shanxi Univ. Sci. Technol.* 39 (04), 130–135. doi:10.3969/j.issn.1000-5811.2021.04.020

Fan, Q., Zhang, Z., and Yin, Y. (2009). *Mechanics of materials*. China: Higher education press.

Gabreil, E., Wu, H., Chen, C., Li, J., Rubinato, M., Zheng, X., et al. (2022). Three-dimensional smoothed particle hydrodynamics modeling of near-shore current flows over rough topographic surface. *Front. Mar. Sci.* 9, 935098. doi:10.3389/fmars.2022.935098

Gong, K., Wu, M., and Liu, G. (2020a). Comparative study on corrosion behaviour of rusted X100 steel in dry/wet cycle and immersion environments. *Constr. Build. Mat.* 235, 117440. doi:10.1016/j.conbuildmat.2019.117440

Gong, K., Wu, M., Xie, F., Liu, G., and Sun, D. (2020b). Effect of dry/wet ratio and pH on the stress corrosion cracking behavior of rusted X100 steel in an alternating dry/wet environment. *Constr. Build. Mat.* 260, 120478. doi:10.1016/j.conbuildmat.2020.120478

Goran, V., Goran, V., Josip, B., Marino, B., and Florian, S. (2021). Long-term marine environment exposure effect on butt-welded shipbuilding steel. *J. Mar. Sci. Eng.* 9 (5), 491. doi:10.3390/jmse9050491

Han, W., Pan, C., Wang, Z., and Yu, G. (2014). A study on the initial corrosion behavior of carbon steel exposed to outdoor wet-dry cyclic condition. *Corros. Sci.* 88, 89–100. doi:10.1016/j.corsci.2014.07.031

Hao, W., Liu, Z., Wu, W., Li, X., Du, C., and Zhang, D. (2018). Electrochemical characterization and stress corrosion cracking of E690 high strength steel in wet-dry

cyclic marine environments. *Mater. Sci. Eng. A* 710, 318–328. doi:10.1016/j.msea.2017.10.042

Jiang, J., Xu, T., and Liu, J. (2021). Study on protection characteristics of D32 steel with different metal coatings in ocean low-salinity wet-dry environment. *Equip. Environ. Eng.* 18 (06), 119–124. doi:10.7643/issn.1672-9242.2021.06.018

Luo, L., Chen, Z., Zhao, X., and Zhang, Y. (2019). Deterioration model for resistance of steel member in atmospheric environment. *Struct. Eng.* 35 (02), 52–58. doi:10.3969/j.issn.1005-0159.2019.02.007

Luo, X., Liu, J., and Nie, J. (2019). Cross-section distribution characteristics and tensile behavior of corroded reinforcing steel bars. *J. Build. Mater.* 22 (05), 730–736. doi:10.3969/j.issn.1007-9629.2019.05.009

Melchers, R. (2020). Long-term durability of marine reinforced concrete structures. *J. Mar. Sci. Eng.* 8 (4), 290. doi:10.3390/jmse8040290

Ming, J., Zhou, X., Jiang, L., and Shi, J. (2022). Corrosion resistance of low-alloy steel in concrete subjected to long-term chloride attack: Characterization of surface conditions and rust layers. *Corros. Sci.* 203, 110370. doi:10.1016/j.corsci.2022.110370

Panteleeva, M. (2017). Effective modern methods of protecting metal road structures from corrosion. *IOP Conf. Ser. Earth Environ. Sci.* 90 (1), 012119. doi:10.1088/1755-1315/90/1/012119

Ren, S., Gu, S., Kong, C., Zeng, S., Gu, Y., Li, G., et al. (2022a). Fractal characteristic of corroded steel surface and application to the fracture analyses. *Constr. Build. Mat.* 340, 127759. doi:10.1016/j.conbuildmat.2022.127759

Ren, S., Kong, C., Gu, Y., Gu, S., Zeng, S., Li, G., et al. (2022b). Measurement pitting morphology characteristic of corroded steel surface and fractal reconstruction model. *Measurement* 190, 110678. doi:10.1016/j.measurement.2021.110678

Shen, L. (2015). *Field testing study on pile hydrodynamic characters of inland river suspended vertical wharf*. China: Chongqing Jiaotong University.

Shi, W., Tong, L., Chen, Y., Li, Z., and Shen, K. (2012). Experimental study on influence of corrosion on behavior of steel material and steel beams. *J. Build. Struct.* 33 (7), 53–60. doi:10.14006/j.jzjgxb.2012.07.006

Song, Z., Wang, Z., Wang, J., Peng, B., and Zhang, C. (2021). Atmospheric corrosion behavior of Q235 steel in northern Hebei region. *Mater. Mech. Eng.* 45 (06), 46–51. doi:10.11973/jxgccl202106008

State Bureau of Technical Supervision GB8923-88 (2011). *Corrosion grade and rust removal grade of steel surface before painting*. China: China Standards Press.

Sultana, S., Wang, Y., Sobey, A., Wharton, J., and Shenoi, R. (2015). Influence of corrosion on the ultimate compressive strength of steel plates and stiffened panels. *Thin-Walled Struct.* 96, 95–104. doi:10.1016/j.tws.2015.08.006

Thee, Ch., Hao, L., Dong, J., Xin, M., Xin, W., Li, X., et al. (2014). Atmospheric corrosion monitoring of a weathering steel under an electrolyte film in cyclic wet-dry condition. *Corros. Sci.* 78, 130–137. doi:10.1016/j.corsci.2013.09.008

Wang, Y., and Cheng, G. (2016). Quantitative evaluation of pit sizes for high strength steel: Electrochemical noise, 3-D measurement, and image-recognition-based statistical analysis. *Mat. Des.* 94, 176–185. doi:10.1016/j.matdes.2016.01.016

Wang, Y., Mu, X., Dong, J., Umoh, A., and Ke, W. (2021). Insight into atmospheric corrosion evolution of mild steel in a simulated coastal atmosphere. *J. Mat. Sci. Technol.* 76, 41–50. doi:10.1016/j.jmst.2020.11.021

Wang, Z., and Liu, Y. (2021). Corrosion behavior and mechanism of carbon steel in typical harsh marine atmosphere in *11th national congress on corrosion and protection* Liaoning: Engineering technology Ⅰ, Special topics in Metal science and metal technology. doi:10.26914/c.cnkihy.2021.015821

Xu, S., and Wang, Y. (2015). Estimating the effects of corrosion pits on the fatigue life of steel plate based on the 3D profile. *Int. J. Fatigue* 72, 27–41. doi:10.1016/j.ijfatigue.2014.11.003

Xu, X., Cheng, H., Wu, W., Liu, Z., and Li, X. (2021). Stress corrosion cracking behavior and mechanism of Fe-Mn-Al-C-Ni high specific strength steel in the marine atmospheric environment. *Corros. Sci.* 191, 109760. doi:10.1016/j.corsci.2021.109760

Zhan, J., Luo, L., and Luo, Y. (2018). "Research on modeling of bearing capacity degradation of corroded components," in The 18th National Symposium on Modern Structural Engineering, Hebei: Cangzhou.

Zhang, X., Chen, Z., Luo, H., Zhou, T., Zhao, Y., and Ling, Z. (2022). Corrosion resistances of metallic materials in environments containing chloride ions: A review. *Trans. Nonferrous Metals Soc. China* 32, 377–410. doi:10.1016/S1003-6326(22)65802-3

Zhang, Y. (2019). *A study on corrosion behavior of Q345q bridge steel in typical atmospheric enviroment in northwest China*. Lanzhou: Lanzhou University of Technology.

Zhao, Z., Mo, S., Xiong, Q., Liu, H., and Liang, B. (2021). Moment capacity of H-section steel beam with randomly located pitting corrosion. *Probabilistic Eng. Mech.* 66, 103161. doi:10.1016/j.probengmech.2021.103161

Zheng, S., Zhang, X., Zhao, X., and Liu, Y. (2018). Experimental and restoring force model research on the seismic behavior of corroded steel frame beams in offshore atmospheric environment. *Eng. Mech.* 35 (12), 98–106+115. doi:10.6052/j.issn.1000-4750.2017.09.0684

Zou, X., Long, J., Chen, Y., Ma, Y., and Wang, L. (2019). Prediction method for resistance degradation of corroded pre-stressed concrete bridges. *J. China & Foreign Highw.* 39 (03), 84–89. doi:10.140848/j.issn.1671-2579.2019.03.016